MSc in Photonics

PHOTONICS**BCN**

Universitat Politècnica de Catalunya (UPC)
Universitat Autònoma de Barcelona (UAB)
Universitat de Barcelona (UB)
Institut de Ciències Fotòniques (ICFO)

http://www.photonicsbcn.eu

Master in Photonics

MASTER THESIS WORK

OPTICAL COHERENCE TOMOGRAPHY WITH A NONLINEAR INTERFEROMETER

Lluc Sendra Molins

Supervised by Prof. Dr. Juan Pérez Torres, (ICFO-UPC)

Presented on date 17th July 2018

Registered at

Escola Tècnica Superior d'Enginyeria de Telecomunicació de Barcelona

Optical coherence tomography with a nonlinear interferometer

Lluc Sendra Molins

ICFO, The Institute of Photonic Sciences, Mediterranean Technology Park, 08860 Castelldefels (Barcelona), Spain

E-mail: lluc.sendra@icfo.eu

Abstract.

We derive what is the signal and the sensitivity of a nonlinear interferometer (Mach-Zehnder or Michelson), that is a novel approach to perform Optical Coherence Tomography (OCT). The physical idea behind this goes back to seminal work done by L. Mandel's group in 1991 [1]. We demonstrate that the use of input coherent light improve the strength of the detected signal in terms of intensity, noise and sensitivity. Finally, we present the counterintuitive differences between considering a single frequency beam or a beam with a certain bandwidth.

Keywords: quantum optics, optical coherence tomography, quantum coherence, nonlinear interferometer.

1. Introduction

Coherence is one of the most fundamental aspects of light, both in quantum and classical theory. It is a physical property of waves which reflects in their capacity to generate high-visibility interference. R. J. Glauber and others [2, 3] developed during the 60's the coherence quantum theory of light.

L. Mandel and colleagues [1, 4, 5] at the 90's developed the idea of induced coherence. The setup proposed consists on two nonlinear crystals forming a Mach-Zenhder interferometer. Each nonlinear crystal can generate a pair of signal-idler photons. Induced coherence of signal photons takes place when the idler photons are indistinguishable. This property has been used by A. Vallés *et al.* [6] to do OCT (see Fig. 1 TOP). The transmissivity of the sample determines the amount of induced coherence observable. This allows to characterize a sample detecting photons that did not interact directly with it.

In a recent experiment, A. V. Petrova *et al.* [7] proposed the same concept using a Michelson interferometer, resulting in a more stable setup as only one nonlinear crystal was used. Furthermore, A. C. Cardoso *et al.* [8] proposed to add a coherent input idler, resulting in stimulated emission (see Fig. 1 BOTTOM).

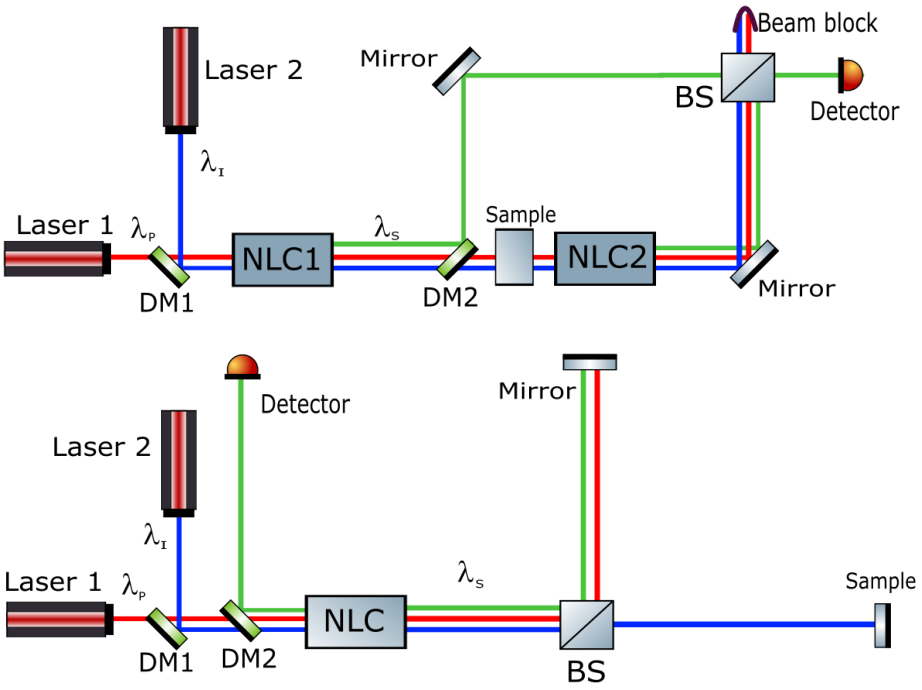

Figure 1. Two different setups of a nonlinear interferometer. The TOP figure is a Mach-Zender interferometer and the BOTTOM one is a Michelson interferometer. Both of them consisting in two lasers (Laser 1 and Laser 2): Laser 1 pumps the nonlinear crystal and Laser 2 is used as an input coherent state for the idler. (NLC: Nonlinear crystal; DM: Dichroic mirror)

There have been extensive analysis of these nonlinear interferometers [6, 7, 8, 9, 10, 11]. Nevertheless, they use different formalisms resulting in a variety of different results. In this work, we synthesize all of these results in a single formalism to compare different setups. Moreover, we use real parameters and extract conclusions to obtain a better characterization of the sample.

2. Current analysis

The interest for nonlinear interferometers has been growing in recent years. Their uses in quantum information and quantum metrology have opened another way to improve the measurements and communications. M. V. Chekhova and Z. Y. Ou have collected the state of the art in nonlinear interferometers, remarking their importance [11].

As already mentioned in Sec. 1, there are many different formalisms to study a nonlinear interferometer. In 2014, G. B. Lemos *et al.* [9] used a formalism that assumes that the probability of generating a pair of photons in the nonlinear interferometer is so small that the generations of two pairs of photons are neglected. This approximation is valid in most of the cases, but it does not allows us to generalize to other regimes.

A. Vallés *et al.* [6] realized a Mach-Zender interferometer and made calculations using the Bogoliuvob's formalism, which uses operators that characterize the nonlinear

optics processes. These operators allow us to generalize the results in every regime, while we are in the non-depleting regime. This formalism is the one that we are going to use in order to collect all the possible cases and compare it.

A. V. Paterova *et al.* [7] proposed, instead of a Mach-Zender interferometer, a Michelson interferometer. The improvement was because they only used one nonlinear crystal, resulting in a more robust setup. On the other hand, A. C. Cardoso *et al.* [8] proposed using a coherent input state for the idler photons, i.e. a laser, to have better results. They obtained a better sensitivity but, once again, they use another formalism: they threat the interferometer in a classical way.

2.1. Bogoliubov's transformations

Bogoliuvob's transformations are unitary transformations which describes the nonlinear process of parametric down-conversion. They are valid when the pump beam is a monochromatic plane-wave (wide beam). In our case, it is useful because it is a good approximation to represent the transformation inside the nonlinear crystals due to the down-conversion process. Therefore, it will be the formalism chosen to analyze the setups.

The transformation is [12]:

$$a_s(\Omega) = U(\Omega)b_s(\Omega) + V(\Omega)b_i^+(-\Omega) \tag{1}$$

$$a_i(\Omega) = U(\Omega)b_i(\Omega) + V(\Omega)b_s^+(-\Omega) \tag{2}$$

where the operators $a_s(\Omega)$ and $a_i(\Omega)$ are the output operators for signal and idler respectively and $b_s(\Omega)$ and $b_i(\Omega)$ are the input operators for signal and idler respectively. Ω is the frequency deviation from the central frequency ($\omega_s = \omega_s^0 + \Omega$) and similarly for the idler wave ($\omega_i = \omega_i^0 - \Omega$). ω_s^0 and ω_i^0 are the central frequencies of the signal and the idler, respectively. The coefficients $U(\Omega)$ and $V(\Omega)$ depend on the spectrum of the generated photons, but they must fulfill that $|U(\Omega)|^2 = 1 + |V(\Omega)|^2$.

In order to get a flavor of the results, we are going to approximate the spectrum as exponentials $\exp\big(-\Omega^2 T_c^2\big)$, where T_c is the coherence time of the beam, that is inversely proportional to the bandwidth of the laser.

3. The signal: visibility of interference

Due to the robustness of the Michelson interferometer and its easier experimental implementation, we are going to analyze it. Nevertheless, the results can be extrapolated to a Mach-Zender interferometer. The operator associated to detected photons in a Michelson's interferometer is

$$d_s(\Omega) = A(\Omega)b_s(\Omega) + B(\Omega)b_i^+(-\Omega) + C(\Omega)f^+(-\Omega) \tag{3}$$

where $b_s(\Omega)$ is the input operator for the signal photon, $b_i(\Omega)$ is the input operator for the idler photon and $f(\Omega)$ is the operator related to the loss on the transmissivity, that

must fulfill $[f, f^+] = 1 - |\tau|^2$. We define $A(\Omega) = U^2(\Omega)\exp(i\phi(\Omega)) + \tau^* V(\Omega)V^*(-\Omega)$, $B(\Omega) = V(\Omega)(U(\Omega)\exp(i\phi(\Omega)) + \tau^* U^*(-\Omega))$, $C(\Omega) = V(\Omega)$. $\phi(\Omega)$ is the phase between the two arms of the interferometer introduced by the difference in the path lengths, which can be expressed as $\phi(\Omega) = \big(\omega_s^0 + \Omega\big)\Delta L/c$, where ΔL is the path-length difference between the two arms. To describe the sample, we model it as a certain transmissivity τ, which gives us which portion of the beam can pass through it.

The number of detected photons is given by:

$$\langle N\rangle = \frac{1}{2\pi}\int_t^{t+T_d} dt' \int_{-\infty}^{+\infty} d\Omega_1 d\Omega_2 \langle d_s^+(\Omega_1) d_s(\Omega_2)\rangle e^{i(\Omega_1-\Omega_2)t'} \tag{4}$$

$$= T_d \frac{1}{2\pi}\int_{-\infty}^{+\infty} d\Omega \left[(1+|\alpha(\Omega)|^2)|B(\Omega)|^2 + (1-|\tau|^2)|C(\Omega)|^2\right] \tag{5}$$

We approximate the spectrum by normalized exponentials, $|C(\Omega)|^2 = 2\sqrt{\pi}RT_c\exp(-\Omega^2 T_c^2)$, $|B(\Omega)|^2 = \big[1 + |\tau|^2 + 2|\tau|\cos(\phi(\Omega) + \phi_\tau)\big]|C(\Omega)|^2$ and $|\alpha(\Omega)|^2 = N_\alpha T_\alpha/\sqrt{\pi}\exp(-\Omega^2 T_\alpha^2)$. Here R is the flux rate of the generated pairs of photons signal-idler, T_c is the bandwidth of the spectrum of the generated ones, T_α is the bandwidth of the laser and N_α is the number of photons generated. Also, we are going to approximate that $\mathrm{sinc}^2\left((\Omega_1 - \Omega_2)T_d/2\right) \approx \exp\left(-(\Omega_1 - \Omega_2)^2 T_d^2\right)$. Using these approximations, we obtain that (see Fig. 2):

$$\langle N\rangle = RT_d t_N(\tau,\phi) + RN_\alpha\sqrt{\pi}\frac{T_c T_\alpha}{\sqrt{T_c^2 + T_\alpha^2}} t_{N_\alpha}(\tau,\phi) \tag{6}$$

where $t_N(\tau,\phi) = 2\left[1 + |\tau|\exp\left(-\left(\Delta L/(2T_c c)\right)^2\right)\cos\left(\omega_s^0\Delta L/c + \phi_\tau\right)\right]$ and $t_{N_\alpha}(\tau,\phi) = 2\Big[1 + |\tau|^2 + 2|\tau|\exp\big(-(\Delta L/(2\sqrt{T_c^2+T_\alpha^2}c))^2\big)\Big]$.

From this expression, we can observe that the number of photons, i.e. the signal that we have to detect, is improved as we increase the power of the input laser.

The visibility is defined as $V = (\langle N\rangle_{max} - \langle N\rangle_{min})/(\langle N\rangle_{max} + \langle N\rangle_{min})$ and is the parameter used to characterize the sample, that in our case is the transmissivity. When we have no input laser ($N_\alpha = 0$) is:

$$V = |\tau| e^{-\left(\frac{\Delta L}{2T_c c}\right)^2} \tag{7}$$

And when we have a laser ($N_\alpha \gg 1$):

$$V = \frac{2|\tau|}{1+|\tau|^2} e^{-\left(\frac{\Delta L}{2\sqrt{T_c^2+T_\alpha^2}c}\right)^2} \tag{8}$$

This is an agreement with the fact that we can obtain maximum visibility when the difference between the paths of the interferometer is minimum. See the visibilities for both cases in Fig. 3.

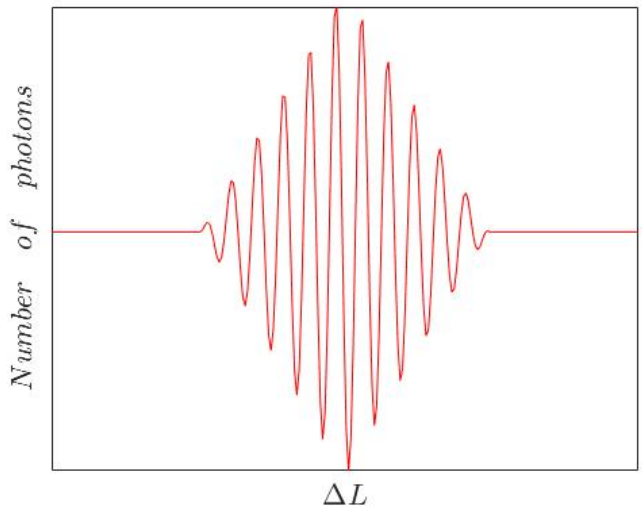

Figure 2. Behavior of the number of photons when we vary the path-length between the two arms of the interferometer.

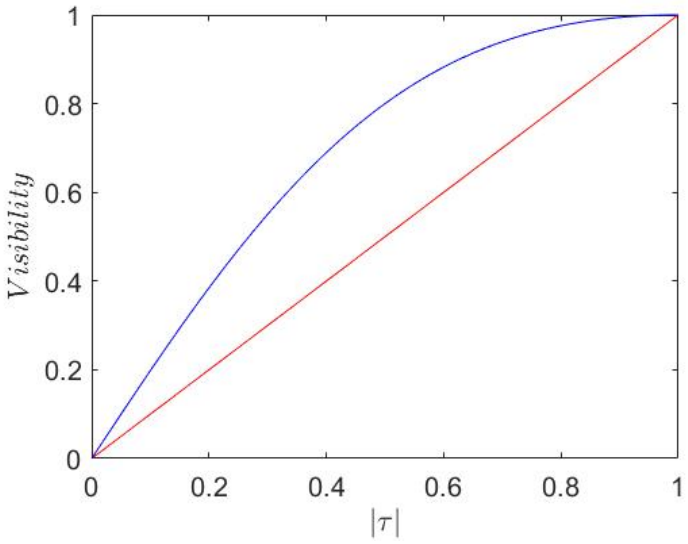

Figure 3. Visibilities as a function of the transmissivity τ, assuming that we have no path difference between the arms of the interferometer ($\Delta L = 0$). The red line is for the case when we do not have any laser. The blue line is when we have a laser.

4. Sensitivity

Apart from the signal itself (number of photons $\langle N \rangle$ and visibility V), it is interesting to take into account other properties of the setup that give us the quality of the signal detected. For the sake of simplicity, we are going to calculate the case when we have no input laser for the idler photons. We define the variance as $\langle \Delta N^2 \rangle = \langle N^2 \rangle - \langle N \rangle^2$, the signal-to-noise ratio (SNR), which gives us an intuition of the quality of the signal, as $SNR = \langle N \rangle / \sqrt{\langle \Delta N^2 \rangle}$, the sensitivity σ, which gives a flavor of how the signal vary

when we varies the sample, as $\sigma = \sqrt{\langle N\rangle}/\left|\partial\langle N\rangle/\partial|\tau|\right|$. We make use of the fact that the transmissivity can be complex ($\tau = |\tau|\exp(i\phi_\tau)$).

To calculate all these properties, we define the coherence function as $C(t', t'') = \langle d_s^+(t') d_s(t'')\rangle$, and taking the Fourier transform of the expected value of the number of photons in the frequency domain, we obtain:

$$C(t', t'') = \frac{1}{2\pi}\int_{-\infty}^{+\infty} d\Omega_1 d\Omega_2 \langle d_s^+(\Omega_1) d_s(\Omega_2)\rangle e^{i\Omega_1 t' - i\Omega_2 t''} \tag{9}$$

$$= \frac{1}{2\pi}\int_{-\infty}^{+\infty} d\Omega \left[|B(\Omega)|^2 + (1-|\tau|^2)|C(\Omega)|^2\right] e^{i\Omega(t'-t'')} \tag{10}$$

Using the previous results, it can be demonstrated that:

$$\langle N^2\rangle = \frac{1}{(2\pi)^2}\int_t^{t+T_d} dt' dt'' \int_{-\infty}^{+\infty} d\Omega \langle d_s^+(\Omega_1) d_s(\Omega_2) d_s^+(\Omega_3) d_s(\Omega_4)\rangle e^{i(\Omega_1-\Omega_3)t' + i(\Omega_2-\Omega_3)t''} \tag{11}$$

$$= \langle N\rangle(\langle N\rangle + 1) + f(T_d) \tag{12}$$

where $f(T_d) = \int_t^{t+T_d} dt' dt'' |C(t', t'')|^2$ and $d\Omega = d\Omega_1 d\Omega_2 d\Omega_3 d\Omega_4$. Then, the variance is:

$$\langle(\Delta N)^2\rangle = \langle N\rangle + f(T_d) \tag{13}$$

In our case, we have that the $f(T_d)$ is:

$$f(T_d) = T_d^2 \frac{1}{(2\pi)^2}\int_{-\infty}^{+\infty} d\Omega_1 d\Omega_2 sinc^2\left(\frac{\Omega_1 - \Omega_2}{2} T_d\right) g(\tau, \Omega_1, \Omega_2) \tag{14}$$

where $g(\tau, \Omega_1, \Omega_2) = |B(\Omega_1)|^2|B(\Omega_2)|^2 + (1-|\tau|^2)\Big[|B(\Omega_1)|^2|C(\Omega_2)|^2 + |C(\Omega_1)|^2|B(\Omega_2)|^2\Big] + (1-|\tau|^2)^2|C(\Omega_1)|^2|C(\Omega_2)|^2$. Using the approximations of Gaussian spectrum that we have already explained, we obtain:

$$f(T) = \frac{\langle N\rangle^2}{\sqrt{1 + 2\left(\frac{\langle N\rangle}{RT_c t_N(\tau,\phi)}\right)^2}} \frac{t_f(\tau,\phi)}{t_N^2(\tau,\phi)} \tag{15}$$

where $t_N(\tau, \phi)$ is defined in Sec. 3 and $t_f(\tau, \phi) = 2t_N(\tau) + |\tau|\cos(\phi + \phi_\tau)\Big[4 + |\tau|\cos(\phi + \phi_\tau)\Big]$. From these results, we can obtain the all the main properties (see Tab. 1). The most important fact of this table is that even we have no input laser, i.e. we have vacuum, we have coherent-like statistics ($SNR = \sqrt{\langle N\rangle}$). To observe the behavior of sensitivity σ, see Fig. 4.

5. Conclusions

In this thesis we have calculated the properties of the Michelson interferometer with the Bogoliubov's formalism, being able to extrapolate it for the Mach-Zender interferometer.

Variable	Expression
$\langle N \rangle$	$4RT_d$
V	$\lvert\tau\rvert$
SNR	$\sqrt{\langle N \rangle}$
σ	$\frac{1}{2\sqrt{\langle N \rangle}}$

Table 1. Properties for a Michelson interferometer. Due to experimental conditions, we use the approximation that $T_d \gg T_c$ and $RT_c \ll 1$. For simplicity, we use that the length difference between the arms is zero ($\phi = 0$) and the transmissivity is maximum and real ($\tau = 1$). The results, in this case, are significant and the results for other values preserve the same behavior. The sensitivity for a PPLN crystal with a bandwidth of $\Delta\lambda = 0.84nm$, a flux rate of generated signal-idler pairs of $R = 5.4GHz$ and a power of signal photons of $P_s = 13pW$ is observed in Fig. 4.

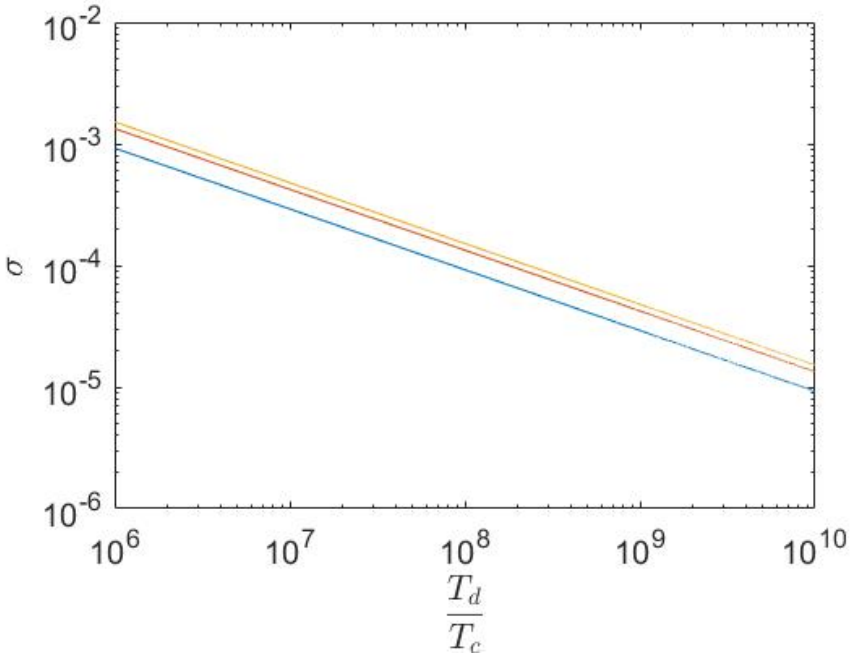

Figure 4. Sensitivity for different values of transmissivity as a function of the ratio between detection and coherence time. We plot the case when the detection time is much bigger than the coherence time $T_d \gg T_c$ since it is the experimental case. BLUE: $\tau = 0.1$. RED: $\tau = 0.7$. YELLOW: $\tau = 1$.

This allows us to compare it, despite of all the other articles presented in Sec. 2, which are in different formalisms. The unification is important because during last years, the interest in nonlinear interferometers is growing, but there is no analysis that allows us to discriminate between the interferometers.

The most important conclusion is that the best interferometer is the Michelson interferometer with a laser input. Accordingly with the results, the best option is to use a laser because it improves the SNR, the sensitivity σ and the detected signal ($\langle N \rangle$) .

The other argument to use a Michelson interferometer is the stability compared

with the Mach-Zender interferometer. This stability is due to the fact that it only uses one nonlinear crystal. Experimentally, nonlinear crystals are difficult to implement, so by reducing the number of nonlinear crystal, we increase the robustness of the setup.

Another conclusion is that the extrapolation of the single-mode case to the multimode case is not trivial. We have observed that the results are different. In fact, for the multimode case, we observe a coherent behavior even when we are in the thermal case.

In order to explain this last phenomena, we do an analysis considering a multimode beam consisting on M single-mode beams. This analysis gives a simple explanation of why the effect explained above happens. The only assumption done is that the different modes are independent. Defining $\langle n_i \rangle$ as the expected number of photons of the i-mode, the total expected number of photons is:

$$\langle N \rangle = \sum_{i=1}^{M} \langle n_i \rangle \tag{16}$$

The squared expected value is:

$$\langle N^2 \rangle = \sum_{i=1}^{M} \left[\langle n_i^2 \rangle + \langle n_i \rangle \sum_{j \neq i, j=1}^{M} \langle n_i^2 \rangle \right] \tag{17}$$

And the variance is:

$$\langle (\Delta N)^2 \rangle = \sum_{i=1}^{M} \langle (\Delta n_i)^2 \rangle \tag{18}$$

With:

$$\langle (\Delta n_i)^2 \rangle = \langle n_i^2 \rangle - \langle n_i \rangle^2 \tag{19}$$

5.1. Coherent state

First of all, we are going to study the case of coherent state, which has the statistics $\langle n_i^2 \rangle = \langle n_i \rangle (\langle n_i \rangle + 1)$ Then, we can obtain that:

$$\langle (\Delta N)^2 \rangle = \langle N \rangle \tag{20}$$

And the signal-to-noise ratio is:

$$SNR = \sqrt{\langle N \rangle} \tag{21}$$

That is the behavior of a coherent state, that is what we expect.

5.2. Thermal state

We are going to use the case of thermal state, which has the statistics $\langle n_i^2 \rangle = \langle n_i \rangle (2\langle n_i \rangle + 1)$ Then, we can obtain that:

$$\langle (\Delta N)^2 \rangle = \langle N \rangle \left(1 + \langle N \rangle \sum_{i=1}^{M} \left(\frac{\langle n_i \rangle}{\langle N \rangle} \right)^2 \right) \tag{22}$$

And the signal-to-noise ratio is:

$$SNR = \sqrt{\frac{\langle N \rangle}{1 + \langle N \rangle \sum_{i=1}^{M} \left(\frac{\langle n_i \rangle}{\langle N \rangle} \right)^2}} \tag{23}$$

An important case for the thermal state is when we have all the modes uniformly distributed, i.e. $\langle n_i \rangle = \langle n \rangle \ \forall i$. In this case, the statistics are given by:

$$\langle (\Delta N)^2 \rangle = \langle N \rangle \left(1 + \frac{\langle N \rangle}{M} \right) \tag{24}$$

And the signal-to-noise ratio is:

$$SNR = \sqrt{\frac{\langle N \rangle}{1 + \frac{\langle N \rangle}{M}}} \tag{25}$$

For the case when we have a large number of photons, which is the usual case, the SNR is finally:

$$SNR = \sqrt{M} \tag{26}$$

What we can observe by this result is that, as we have more modes, we have a better SNR. So the more modes, the better the interferometer is. Then, the behavior is different if we consider the multimode case instead of the single-mode.

Acknowledgments

First of all, my great appreciation goes to my supervisor, Prof. Dr. Juan Pérez Torres, for giving me the opportunity to study in his quantum optics group at ICFO during the last year. I would also like to acknowledge Gerard Jiménez and my office mates Juan Rafael Alvarez and Verónica Vicuña for the scientific and non-scientific conversations. I also want to thank to my group mates Dorilian López and Isael Herrera for making ICFO a nice and pleasant place. Finally, I would like to acknowledge Prof. Dr. S. Barnett for its illustrative contributions.

Bibliography

[1] X. Y. Zou, L. J. Wang, and L. Mandel, "Induced coherence and indistinguishability in optical interference," *Physical Review Letters*, vol. 67.7, pp. 318–321, 1991.

[2] R. J. Glauber, "The quantum theory of optical coherence," *Physical Review*, vol. 130.6, pp. 2529–2539, 1963.

[3] R. J. Glauber, "Coherent and incoherent states of the radiation field," *Physical Review*, vol. 131.6, pp. 2766–2788, 1963.

[4] Z. Y. Ou, L. J. Wang, X. Y. Zou, and L. Mandel, "Evidence for phase memory in two-photon down conversion through entanglement with the vacuum," *Physical Review A*, vol. 41.1, pp. 566–568, 1990.

[5] X. Y. Zou, T. P. Grayson, G. A. Barbosa, and L. Mandel, "Control of visibility in the interference of signal photons by delays imposed on the idler photons," *Physical Review A*, vol. 47.3, pp. 2293–2295, 1993.

[6] A. Vallés, G. Jiménez, L. J. Salazar-Serrano, and J. P. Torres, "Optical sectioning in induced coherence tomography with frequency-entangled photons," *Phys. Rev. A*, vol. 97, p. 023824, Feb 2018.

[7] A. V. Paterova, H. Yang, C. An, D. A. Kalashnikov, and L. A. Krivitsky, "Tunable optical coherence tomography in the infrared range using visible photons," *Quantum Science and Technology*, vol. 3, no. 2, p. 025008, 2018.

[8] A. C. Cardoso, L. P. Berruezo, D. F. Ávila, G. B. Lemos, W. M. Pimenta, C. H. Monken, P. L. Saldanha, and S. Pádua, "Classical imaging with undetected light," *Phys. Rev. A*, vol. 97, p. 033827, Mar 2018.

[9] G. B. Lemos, V. Borish, G. D. Cole, S. Ramelow, R. Lapkiewicz, and A. Zeilinger, "Quantum imaging with undetected photons," *Nature*, vol. 512, p. 409, 2014.

[10] J. H. Shapiro, D. Venkatraman, and F. N. C. Wong, "Classical imaging with undetected photons," *Scientific Reports*, vol. 5, p. 10329, 2015.

[11] M. V. Chekhova and Z. Y. Ou, "Nonlinear interferometers in quantum optics," *Adv. Opt. Photon.*, vol. 8, pp. 104–155, Mar 2016.

[12] J. P. Torres, K. Banaszek, and I. A. Walmsley, "Engineering nonlinear optic sources of photonic entanglement," *Progress In Optics*, vol. 56, pp. 227–331, 2011.